DØ Note 2911
04/12/96

Effects of Radiation on the Leakage Currents of Silicon Microstrip Detectors for the H and F-Disks of the DØ Silicon Tracker

R. Gómez, Fermilab, Batavia, IL 60510
A. Bischoff, C. Boswell, J. Ellison, University of California, Riverside, CA 92521
P. Gutierrez, G. Guglielmo, University of Oklahoma, Norman, OK 73019
W. Cooper, M. Johnson, R. Lipton, S. Mishra, P.A. Rapidis, L. Spiegel, Fermilab, Batavia, IL 60510

Abstract

This is a report on the irradiations of H and F-disk detectors performed during January and February 1996 at the Fermilab Irradiation Facility. It was found that the current design of the F-disk double sided detectors (15° stereo), with only one guard ring on each side, is extremely sensitive to radiation. The guard ring and bias currents become very large after doses of less than 100 Krad, with the guard ring current reaching the milliampere level. This dramatic increase in currents is thought to be caused by surface damage (i.e. charge accumulation in the SiO_2-Si interface) although no firm evidence for this claim exists. This damage anneals very fast, causing the currents to decrease by 70% to 90% in 33 hours. These results are compared with those of multiguard detectors and test structures, which show much lower currents after irradiation, leading to the conclusion that a multiguard structure may be the solution to the high currents observed in DØ's F-disk detectors. The H-disk prototype detector started with very high leakage currents which also reached the milliampere level after exposure to a fluence much lower than that expected during Run II.

1. INTRODUCTION

This report is part of an ongoing effort to study the effects of radiation on the Silicon Tracker that will be part of the DØ Detector Upgrade. The damage caused by radiation affects the main operation parameters of silicon detectors, resulting in the increase of full depletion voltage, increase in leakage currents, decrease in interstrip isolation, etc.. In this note we will present some of the experimental data obtained after three irradiation tests of silicon detectors in which the change in leakage currents was measured. These irradiations were performed on two sets of DØ's detectors manufactured by Micron Semiconductor (mainly wedges for the F-disks) and a set of detectors and test structures from the ATLAS experiment at the LHC.

During the irradiation performed at TRIUMF in may 1995 the leakage currents of the wedge prototypes raised dramatically, from the microampere level to the milliampere level, after doses smaller than 100 Krad. At that moment it was impossible to know if the current was coming from the bias line or the guard ring because the two lines were connected together and only the total current was being measured. In an attempt to understand this phenomenon, the main focus of these tests were the leakage currents, verifying what was observed at TRIUMF and comparing the behavior of DØ's wedges with that of other detectors with different guard ring structures.

Due to several problems encountered during the irradiations the estimated fluences have very large errors, so caution must be exercised when trying to compare the results presented here with any other experiment. It is recommended to interpret the data in a qualitative way because the uncertainties involved make very difficult to extract solid quantitative results.

2. IRRADIATION PROCEDURES

All these irradiations were performed at the Fermilab Irradiation Facility, located in one of the Booster's beam dump lines (identified as the AP-4 line). This line provides a pulsed beam of 8 GeV protons with intensities than can be adjusted from approximately 10^9 to 4×10^{12} protons per pulse and pulse intervals from 2.9 s to 200 s. The operation modes of the beam line are given in the following sub-sections. The dose monitoring is accomplished on-line by a toroid and off-line by the analysis of the activation of Al foils placed in front or behind the detectors. Unfortunately during the first February irradiation of 1996 no foils were used and because of problems with the toroid readings the uncertainty in the fluence is very large. Another factor that increases the errors in the fluence is the stray flux coming from the beam line when it is being used to dump high intensity beam.

The proton fluences quoted here are not normalized to 1 MeV neutron fluences, as is customary for radiation damage studies, because the spectra and contamination of the proton beam are not known. Assuming a pure and monoenergetic 8 GeV proton beam, the equivalent 1 MeV neutron fluence $\Phi_n(1\,\mathrm{MeV})$ can be calculated as the proton fluence $\Phi_p(8\,\mathrm{GeV})$ times the ratio of the displacement kerma cross sections for both particles at those energies:

Disp. Kerma Cross Section for 8 GeV protons (from [1]): $D_p(8\ \text{GeV}) \cong 8.0 \times 10^4\ \text{eV} \cdot \text{barn}$

Disp. Kerma Cross Section for 1 MeV neutrons (from [2]): $D_n(1\ \text{MeV}) \cong 9.5 \times 10^4\ \text{eV} \cdot \text{barn}$

$$\Phi_{ne}(1\ \text{MeV}) = \frac{D_p(8\ \text{GeV})}{D_n(1\ \text{MeV})} \times \Phi_p(8\ \text{GeV}) \cong 0.84 \times \Phi_p(8\ \text{GeV}) \quad (1)$$

The detectors are located in a gas and light tight aluminum box, whose temperature can be controlled, inside which dry nitrogen is circulated to keep the humidity as low as possible (the humidity is not measured). This box is mounted on a X-Y movable table that enables us to take the detectors out of the beam and sweep the detectors across the beam as will be described later.

All leakage currents mentioned from now on were measured, unless otherwise stated, at 60V bias, and normalized to 20°C according to the following relation [3]:

$$I(T_2) = I(T_1) \cdot e^{\frac{-E \cdot (T_1 - T_2)}{kT_1T_2}}, \quad (2)$$

where k is the Boltzmann constant and E = 0.64 eV.

2.1. January Exposure

Starting on January 21 the following detectors were irradiated:

- F-disk detector (wedge) No. 1295-15:
  - Manufactured by Micron Semiconductor.
  - Double sided, 15° stereo, single guard ring.
  - New Batch, n-side p-stop implant dose = 5×10^{14} cm^{-2}.
- F-disk detector (wedge) No. 969-15:
  - Manufactured by Micron Semiconductor.
  - Double sided, 15° stereo, single guard ring.
  - Old Batch, n-side p-stop implant dose = 2×10^{13} cm^{-2}.
- H-disk detector No. H-10:
  - Manufactured by Moscow State University.
  - Single sided, single guard ring.

The detectors were kept at 10°C in a dry N_2 atmosphere during the exposure. The bias voltage was 60V except at the times when VI curves were being taken. For the double sided detectors the n-side bias line and guard ring were connected together to the power supply (at 60V) and the p-side bias and guard currents to ground were measured during the whole exposure. The H-disk detector had the bias line and the guard ring connected together.

A fluence of $(2 \pm 1)\times10^{13}$ protons/cm^2 (534 ± 267 Krad) was achieved after 3 irradiation periods, from January 21 to January 27. Because the beam is much smaller than the detector area (beam $\sigma\approx3$ mm) the detectors were moved over the beam according to a 8.4 cm × 3.6 cm (hor. × vert., 30.24 cm^2) grid with 0.4 cm steps. At each point of the grid the full dose was applied by delivering approximately 120 beam pulses of 2.6×10^{10} protons each, with pulses every 2.9 seconds. This fluence was estimated using the beam toroid readings and Al foils, but has very large errors due to a misalignment of the detectors with respect to the beam.

Unfortunately the dose was not applied uniformly over the detector area due to a misalignment of the moving table. As Figure 1 shows, only 50% of the detector area was directly hit by the beam. All doses quoted for this exposure are calculated using the area of the irradiated region, not the detector area. This means that 50% of the detector received the quoted dose and the rest received less than 15% of that.

2.2. First February Exposure

In the first irradiation performed on February the following detectors were exposed:

- F-disk detector (wedge) No. 1295-25:
  - Manufactured by Micron Semiconductor.
  - Double sided, 15° stereo, single guard ring.
  - New Batch, n-side p-stop implant dose = 5×10^{14} cm^{-2}.
- F-disk detector (wedge) No. 938-18:
  - Manufactured by Micron Semiconductor.
  - Double sided, 15° stereo, single guard ring.
  - Old Batch, n-side p-stop implant dose = 2×10^{13} cm^{-2}.
- Barrel detector No. 1267-10a:
  - Manufactured by Micron Semiconductor.
  - Single sided, single guard ring.

The detectors were kept at 5°C in a dry N_2 atmosphere during the exposure. The bias voltage was 60V except at the times when VI curves were being taken. For the double sided detectors the n-side bias line and guard ring were connected together to the power supply (at 60V) and the p-side bias and guard currents to ground were measured during the whole exposure. The single sided detectors were connected in a similar fashion.

A fluence of $(5.2 \pm 1.3)\times10^{12}$ protons/cm^2 (139 ± 35 Krad) was delivered during 3 irradiation periods, from February 7 to February 11. Because the beam is much smaller than the detector area (beam $\sigma\approx3$ mm) the detectors were moved over the beam according to a 8 cm × 6 cm (hor. × vert., 48 cm^2) grid with 0.2 cm steps. At each point of the grid a dose of approximately 25 Krad was delivered per grid sweep, giving an average rate (for the whole area) of 2.2 Krad/hour. This fluence was estimated using only the beam toroid readings and has very large errors due to

problems with the instruments and because, even when the detectors were out of the beam, they received large stray fluxes from the beam (i.e. during "shot setup" in the Tevatron), which could not be measured with the toroid.

2.3. Second February Exposure

From February 16 to February 22 the following detectors were irradiated:

- SI prototype detectors (wedges) Nos. SI-26 and SI-41:
  - Manufactured by SINTEF.
  - Size similar to those of DØ.
  - Double sided, multiple guard ring.
- Atlas prototype detector:
  - Manufactured by Micron Semiconductor.
  - Square, 6 cm × 6 cm.
  - Semi-double sided (fully functional n side, p-side plane instead of strips), 4 guard rings on each side.
- Atlas test structure No. TS-1:
  - Manufactured by Micron Semiconductor.
  - Square, active area of 0.5 cm × 0.5 cm.
  - Double sided, 11 guard rings.
- Atlas test structure No. TS-2:
  - Manufactured by Micron Semiconductor.
  - Square, active area of 0.5 cm × 0.5 cm.
  - Double sided, 9 guard rings.

The detectors were kept at 5°C in a dry N_2 atmosphere during the exposure. The bias voltage was 60V except at the times when VI curves were being taken. For the double sided detectors and test structures the n-side bias line and inner guard ring were connected together to the power supply (at 60V) and the p-side bias and inner guard currents to ground were measured during the whole exposure. For the semi-double sided Atlas detector the p-side bias plane and inner guard ring were connected together to the power supply (at 60V) and the n-side bias and inner guard currents to ground were measured during the whole exposure. All guard rings, except the inner ones, were left floating in all detectors.

A fluence of $(7.89 \pm 1.26)\times10^{12}$ protons/cm^2 (211 ± 37 Krad) was delivered during 4 irradiation periods, from February 16 to February 22. This fluence was determined by the activation analysis of an Al foil located in the center of the exposed region. Because the beam is much smaller than the detector area (beam $\sigma\approx3$ mm) the detectors were moved over the beam according to a 8 cm × 6 cm (hor. × vert., 48 cm^2) grid with 0.2 cm steps. At each point of the

grid a dose of approximately 25 Krad was delivered per full grid sweep, giving an average rate (for the whole area) of 2.9 Krad/hour.

3. RESULTS

3.1. January Exposure

Note: All fluences and doses quoted in this section have an error of ±50% unless otherwise noted.

During this exposure the wedges' guard currents were seen to increase dramatically after a small dose. Unfortunately the measurements from this irradiation are of very low quality because, as was mentioned before, the dose monitoring did not work properly and the beam was misaligned. In spite of this we consider it interesting to show a collection of VI curves for each detector at different fluences (see Figure 2 through Figure 4), which is enough to see how sensitive the wedges are.

This was the first time an H-disk detector (No. H-10) was irradiated and it also demonstrated to be fairly susceptible to radiation. As Figure 2 illustrates, at the end of the irradiation the total (bias+guard) current was 1.1 mA. Note that the initial current was 51 μA, which is already high for a non-irradiated detector (currents measured at 60V bias).

Trying to understand the origin of such large currents in the F-disk detectors, the guard ring voltage with respect to the bias line was varied, while the bias voltage was kept constant, and the currents were measured (see Figure 5). It is still not clear what this curves could tell us about the nature of the damage. The most simple explanation would be that the guard current is going from the n-side to the p-side around the edge through surface channels on each side and, as the voltage between the n-side and the p-side guard rings decreases, so does the current. The channels can be formed by radiation induced charge trapped in the interface between the bulk n-silicon and the SiO_2 layer. This kind of damage could equally appear in the single sided barrel detectors but it has been confirmed that their currents remain low.

The fact that the guard ring floats at a voltage much lower than the bias voltage (see the voltages at which the guard current is zero in Figure 5a) suggests that the depletion region extends well beyond the guard. As the effective doping concentration decreases, the depletion region extends and approaches the edge, where crystal damage provides increased current generation rates [4]. Again, this explanation is not consistent with the differences observed between single and double sided detectors.

On the other hand, the dramatic increase in guard ring current with bias voltage (almost as a forward biased junction) may point to a breakdown of the depletion region around the guard ring. This kind of mechanism would be dependent on the geometry of the guard ring, thus explaining the different behavior of the single sided detectors. However, there is no further evidence to support this claim.

3.2. First February Exposure

Note: All fluences and doses quoted in this section have an error of ±25% unless otherwise noted.

Because the detectors are very different in size, for some of the figures and calculations the bias currents were normalized with the active volume and the guard currents with the guard ring length (perimeter). The guard current is not normalized with volume because it is very difficult to know the volume of the region where it is generated and, what is more important, it is very likely that it is not be generated by a volume dependent mechanism. With this normalization the currents from detectors of different size can be directly compared, although normalized guard currents cannot be compared to normalized bias currents.

The behavior of DØ's wedges' leakage currents observed during the January irradiation were reproduced in this exposure, as Figure 6 illustrates. While the barrel detector's total current reached around 0.1 mA after 5.2×10^{12} protons/cm^2 (139 Krad), the wedges' total currents increased to approximately 6 mA. The large variations in the wedges' currents are caused by their extreme sensitivity to radiation and their fast annealing during the periods when the beam was off (see section 3.2.1). Upon turning the beam on, some of the currents raised very fast, reaching a plateau which increased with fluence, at a slow rate. In other words, there is a fast component that seems to saturate superimposed on a slow component that is not significantly different from the damage observed in the barrel detectors (see Figure 7 through Figure 10). These currents appear in the figures as having started at very high levels because the fast initial increase, at low fluences, was not properly recorded.

The lines in Figure 7 through Figure 10 correspond to least square fits to the points where the dose appears to be best measured and the slope of the fits will be used as a figure of merit (damage rate) to compare the performance of different detectors. These damage rates represent the increase in current per unit volume (or length) per unit fluence, without compensating for annealing. They are different from the "damage constant" that is standard in radiation damage studies. The main differences are that we normalized the guard currents with length instead of volume, the "damage constant" is calculated for long term damage compensated for annealing and with fluences that are normalized to 1 MeV neutrons.

Because these damage rates are greatly affected by the fast variations that the wedges' currents show, two damage rates are presented in Table 1: A long term damage rate calculated for a large fluence interval, covering almost the whole exposure and smoothing out the variations (Figure 7 and Figure 8); and a short term damage rate calculated for a particular fluence interval where the fast damage component is clearly visible (Figure 9 and Figure 10). The long term damage rates calculated for these detectors, from data points covering almost the whole exposure, are given in Table 1. It is clear from the table that the wedges' guard ring currents are extremely sensitive, with damage rates one and two orders of magnitude larger than the barrel's damage rates.

Detector	*Long Term* Bias Dam. Rate [A/m]	*Long Term* Guard Dam. Rate [A.cm]	*Short Term* Bias Dam. Rate [A/cm]	*Short Term* Guard Dam. Rate [A.cm]
1267-10a (barrel)	6×10^{-17}	2×10^{-19}	8×10^{-17}	3×10^{-19}
938-18 (old wedge)	6×10^{-17}	5×10^{-17}	7×10^{-16}	4×10^{-16}
1295-25 (new wedge)	2×10^{-17}	4×10^{-17}	5×10^{-17}	4×10^{-16}

Table 1: Long and short term damage rates calculated according to the fits shown in Figure 7 through Figure 10.

3.2.1. Annealing

Annealing of the wedges' currents is very fast (see Figure 11), decreasing by 70% to 90% in 33 hours, while the barrel's bias current decreased only 10% during the same time. The barrel's guard current showed almost no annealing and was not included in the figure.

It is very interesting to see how similar is the annealing of both currents of detector 938-18, even though their magnitudes differ by more than a factor of 10. This may suggest that the same mechanism is generating both currents, although this is very unlikely. A better explanation would be that the large guard current is coupling to the bias line. The clear difference between the annealing of the barrel detector and that of the wedges indicates that while the barrel's current is mainly generated by bulk damage, the wedges' currents come from other process (or processes). The 1295-25 guard current shows very sharp changes in behavior at several times. Those changes could be caused by the ending and starting of different annealing processes.

The annealing of the guard current of detector 1295-25 was parametrized in two different ways. Both fits use the following function:

$$I(t) \cong I(t=0)\cdot\left(A_1\cdot e^{\frac{-t}{\tau_1}} + A_2\cdot e^{\frac{-t}{\tau_2}}\right) \tag{3}$$

The first fit does not take into account the changes in behavior and uses parameters independent of time (see "Single Fit" in Figure 12) and the second fit uses five different sets of parameters, one for each time interval where the behavior changes (see "Multiple Fit"in Figure 12). Table 2 shows the parameters calculated with a least square method. If one is interested only in the long term annealing, the single fit is good enough.

The fast rise and annealing of the wedges' guard currents can also hold the clue to understanding the nature of the damage and why it is so different to that observed on the single sided barrel detectors. However, we must again remark that the phenomenon is not yet understood.

Time Interval	A_1	τ_1 [hours]	A_2	τ_2 [hours]
Single Fit: t > 0	0.81	4.33	0.19	77.01
Multiple Fit:				
(A) $0 \le t \le 0.42$ hrs.	1.00	16.46	0	-
(B) $0.42 < t \le 2.39$ hrs.	0.92	47.30	0.42	0.24
(C) $2.39 < t \le 7.27$ hrs.	3.13	1.04	0.79	7.52
(D) $7.27 < t \le 11.22$ hrs.	8.70×10^{3}	0.61	0.25	∞
(E) t > 11.22 hrs.	6.32	2.49	0.20	67.88

Table 2: Parameters calculated for the annealing of the guard current of detector 1295-25, irradiated in the first February exposure, according to the fits shown in Figure 12.

3.3. Second February Exposure

Note: All fluences and doses quoted in this section have an error of ±16% unless otherwise noted.

As can be seen in Figure 13 through Figure 15, the Atlas detector and test structures show a linear increase in guard and bias current, and the rate of increase is not as dramatic as that observed in the DØ F-disk detectors. On the other hand, the SI detectors' (SI-26 and SI 41) currents increase, in a non linear way, to the milliampere level with fluences as low as 1×10^{12} protons/cm^2 (27 Krad), much like DØ's wedges. A striking feature of the SI detectors is the *decrease* in bias current with fluence.

The Atlas detector and test structures present an almost linear increase in current with fluence and after normalization with size the currents are very similar in magnitude, except for the test structure TS-1 which has a higher guard current (by a factor of 3). By fitting straight lines to the Atlas detector normalized currents, as a function of fluence, we obtain the following long term damage rates:

Atlas Long Term Bias Current Damage Rate: $\alpha_{bias}=6.9\times10^{-17}$ A/cm

Atlas Long Term Guard Current Damage Rate: $\alpha_{guard}=1.7\times10^{-19}$ A.cm

It should be noted that, as Figure 13 shows, both currents differ only by a factor which is independent of the fluence. This may be an indication that in the Atlas detector (and test structures) the bias and guard current are generated mainly by bulk damage.

The SI detectors (SI-26 and SI-41) had very large initial currents and exhibited a strange behavior with irradiation. Their guard currents become very large (on the order of milliamps) after a fluence of approximately 1×10^{12} protons/cm^2 (27 Krad) and the bias currents decrease (!!!) in an exponential way after having increased dramatically at the beginning of the exposure. Figure 16 shows the SI bias currents normalized with detector volume and fitted, with a least square method, to the following functions:

$$I_{SI-26}(\Phi) \cong 9.9\times10^{-4}\,\mathrm{A\cdot cm^{-3}}\cdot e^{-1.6\times10^{-12}\,\mathrm{cm^2}\cdot\Phi} + 1.7\times10^{-4}\,\mathrm{A\cdot cm^{-3}}, \quad (4)$$

$$I_{SI-41}(\Phi) \cong 1.7\times10^{-3}\,\mathrm{A\cdot cm^{-3}}\cdot e^{-1.1\times10^{-12}\,\mathrm{cm^2}\cdot\Phi} + 1.7\times10^{-4}\,\mathrm{A\cdot cm^{-3}}, \quad (5)$$

for: 7.6×10^{11} protons/cm^2 ≤ Φ ≤ 7.9×10^{12} protons/cm^2.

The annealing of all the currents was slow, compared to that observed in DØ's wedges, decreasing by 10% to 20% in 100 hours at 5°C, except for the SI-41 guard current which decreased by 60% and the TS-1 guard current which increased 5% in the same time.

Figure 17 illustrates the changes in the VI curves of the Atlas detectors during the irradiation. Compare them with the VI curves of the wedges irradiated in January.

4. EXPECTED DOSE FOR THE F-DISKS

In DØ Note 2679 [5] the charged particle and neutron fluxes during Run II was estimated. For the F-disks we will use half the charged particle flux because the low momentum particles will not traverse the disks more than once as they do with the barrels. Hence, the charged particle flux is given by:

$$\phi_{ch}(r_\perp) \cong \frac{5.95\times10^{10}}{r_\perp^2}\,\mathrm{cm^{-2}/pb^{-1}} \quad (6)$$

where $r_\perp$ is the distance perpendicular to the beam direction. If we integrate this flux over the whole disk coverage (from an inner radius of 2.54 cm to an outer radius of 9.84 cm) and divide by the area, we get the following average flux:

$$\phi_{ch} \cong 2.6\times10^{9}\,\mathrm{cm^{-2}/pb^{-1}}$$

And the neutron flux is:

$$\phi_{n} \cong 1.8\times10^{9}\ \mathrm{cm^{-2}/pb^{-1}} \quad (7)$$

This means that with the Tevatron running at an approximate integrated luminosity of 2000 pb^{-1}/year [5] the fluences will be:

$$\phi_{ch} \cong 5.2\times10^{12}\ \mathrm{cm^{-2}/year} \quad (8)$$

for charged hadrons, and

$$\phi_{n} \cong 3.6\times10^{12}\ \mathrm{cm^{-2}/year} \quad (9)$$

for neutrons.

These fluxes are accurate to within a factor of 2 because they do not take into account other particles, like gammas, electrons, etc. and processes like beam-gas collisions or Tevatron beam losses.

5. CONCLUSIONS

During the first two exposures performed in 1996, the F-disk detectors showed to be extremely sensitive to radiation. Their guard ring currents reach the milliampere level after doses smaller than 100 Krad, which are much lower than the dose expected during Run II. The damage has two components, a dominant fast component that saturates after a small fluence and a slow component which keeps increasing with fluence. The mechanism producing such large currents is yet unknown but the most simple explanation would be that the guard current is going from the n-side to the p-side around the edge through surface channels on each side. Also the fact that the guard ring floats at a voltage much lower than the bias voltage suggests that the depletion region extends well beyond the guard. As the effective doping concentration decreases, the depletion region extends and approaches the edge, where crystal damage provides increased current generation rates. This kind of damage could equally appear in the single sided barrel detectors but it has been confirmed that their currents remain low. On the other hand, the dramatic increase in guard ring current with bias voltage (almost as a forward biased junction) may point to a breakdown of the depletion region around the guard ring. This kind of mechanism would depend on the geometry of the guard ring, thus explaining the different behavior of the single sided detectors. However, there is no further evidence to support this claim.

It should be pointed out that the annealing observed on DØ's wedges, with time constants on the order of hours, is much faster than that reported for experiments on surface damage [7], where the charge accumulation on the SiO_2-Si interface was measured.

The most important conclusion that we can draw from these tests is that the current F-disk detector design is not radiation hard and the problems observed could be solved by using a multiple guard ring structure. This statement is based on the assumption that any other differences, besides the multigard structure, between DØ's wedges and the Atlas detector and test structures are small and irrelevant to the radiation hardness. However, with the data we have it is not possible to support or deny this assumption.

During the first January irradiation there seemed to be a difference in behavior between the old and new wedge batches, with the new detector (1295-15) being more sensitive than the old one (969-15), but in the first February irradiation the old one (938-18) had larger currents than the new one (1295-25). The only known difference between the two batches is the n-side p-stop implantation dose but this is, in principle, not relevant to the currents we are measuring because of the way the bias lines and guard rings were connected.

This was the first time that an H-disk detector was irradiated and it appears to be fairly sensitive. Its total current (bias + guard) reached 2 mA after a fluence of $(2 \pm 1)\times10^{13}$ protons/cm^2 (534 ± 267 Krad). During Run II these detectors should be able to withstand a flux of 1.1×10^{12} cm^{-2}/year from charged particles alone [8], with the

collider running at an integrated luminosity of 2000 pb^{-1}/year [6]. Further testing should be performed to confirm the observed behavior and find ways to enhance the design.

We thank the Fermilab Accelerator Division, specially Jim Lackey and the Booster personnel for their invaluable help in comissioning and running the irradiation facility.

6. REFERENCES

[1] A. Van Ginneken, "Non Ionizing Energy Deposition in Silicon For Radiation Damage Studies," *FN-522*, October 1989.

[2] ASTM Standard E722-85, Annual Book of ASTM Standards, Vol. 12.02, p. 328, 1985.

[3] L. Evensen *et al.*, "Guard Ring Design for High Voltage Operation of Silicon Detectors," *Nucl. Instrum. Methods*, vol. A337, pp. 44-52, 1993.

[4] J.A. Ellison, A.P. Heinson, "Effects of Radiation Damage on the DØ Silicon Tracker," *DØ Internal Note 2679*, July 1995.

[5] S. Mishra, "Tevatron Luminosity," *Fermilab WWW Site*, http://www-fermi3.fnal.gov/luminosity-table.html, June 1995.

[6] D.D. Pitzl *et al.*, "Study of Radiation Effects on AC-Coupled Silicon Strip Detectors," *Nuclear Physics B (Proc. Suppl.)*, vol. 23A, pp. 340-346, 1991.

[7] E. Shabalina, V. Sitorenko, "Radiation Damage Effects on the Forward H-Disks of DØ Silicon Tracker," *DØ Note 2800*, November 1995.

[8] R. Gómez *et al.*, "Studies of Radiation Damage in Silicon Microstrip Detectors for the DØ Silicon Tracker," *DØ Note 2816*, September 1995.

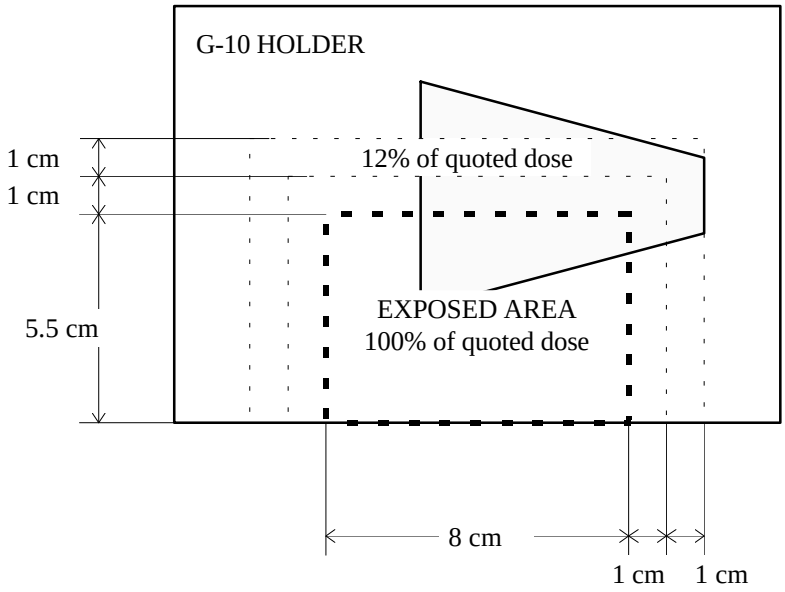

Figure 1: Beam misalignment during January/96 irradiation.

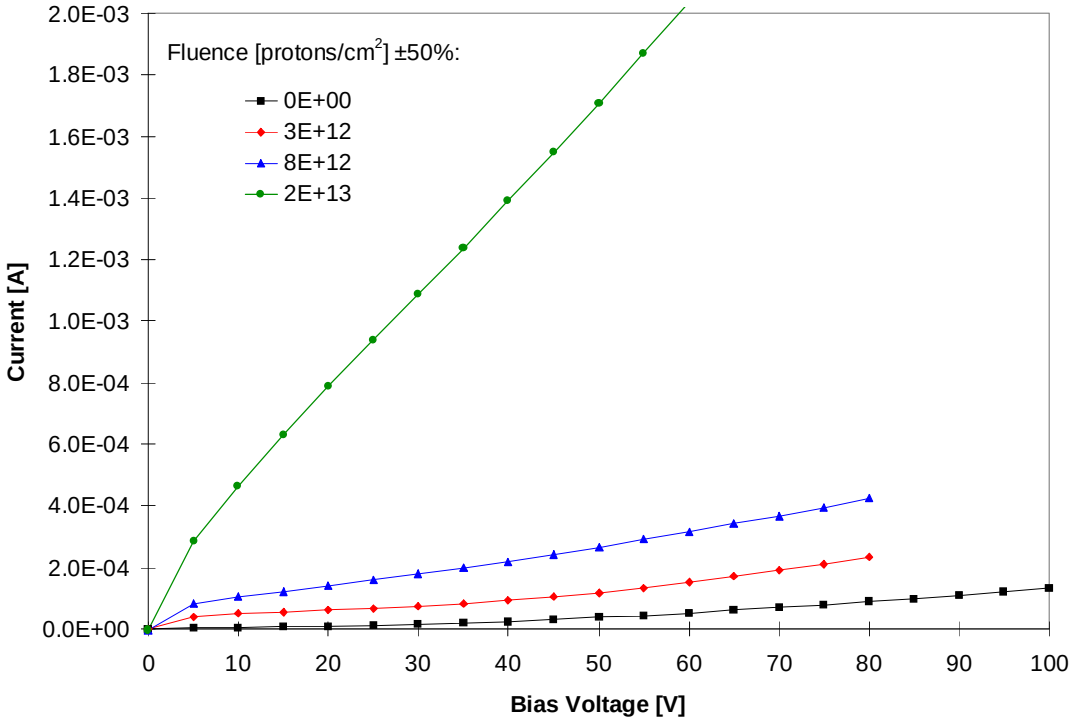

Figure 2: H-disk detector H-10 VI curves (bias+guard) for different fluences.

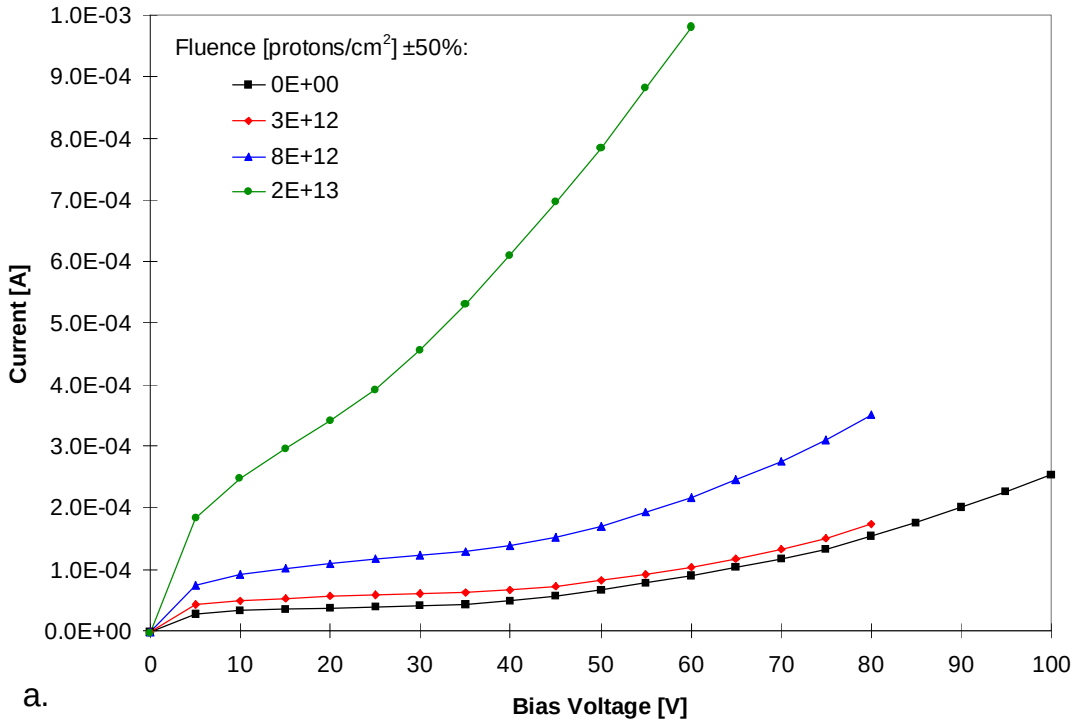

a.

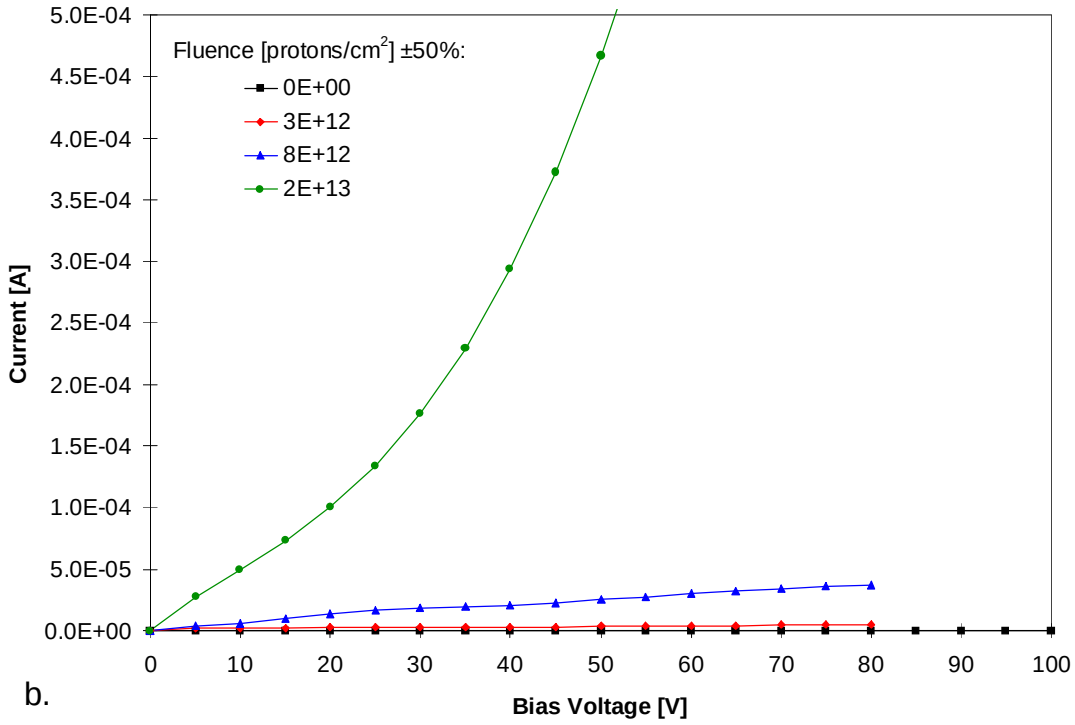

b.

Figure 3: F-disk detector 969-15 VI curves for different fluences. a) Bias current. b) Guard ring current.

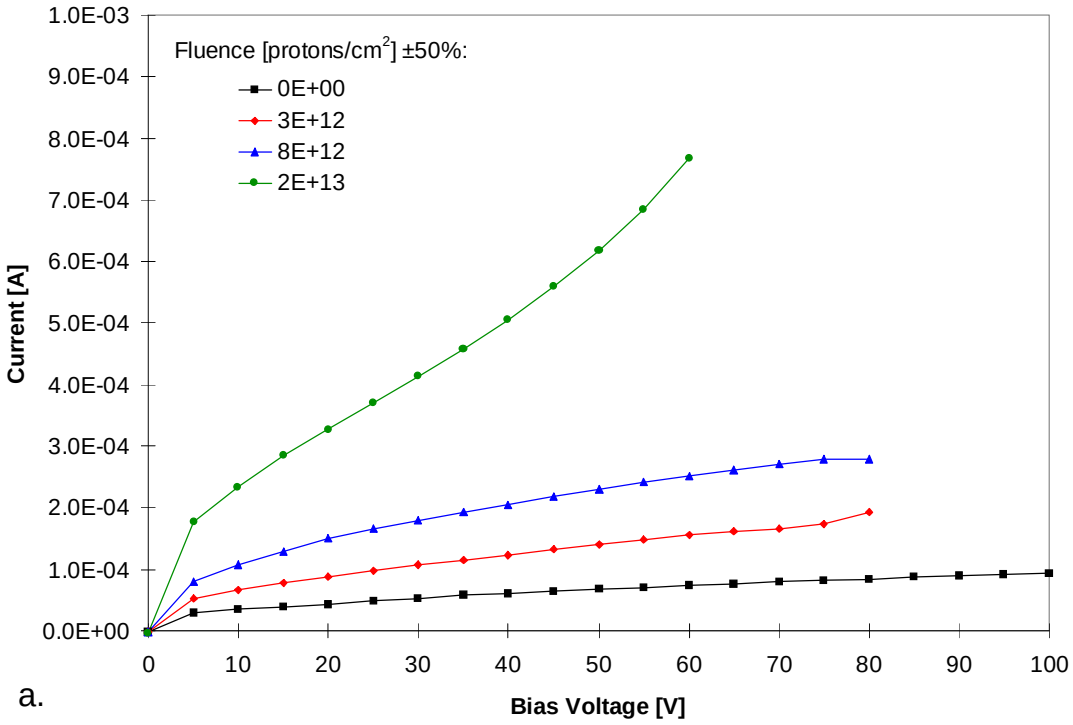

a.

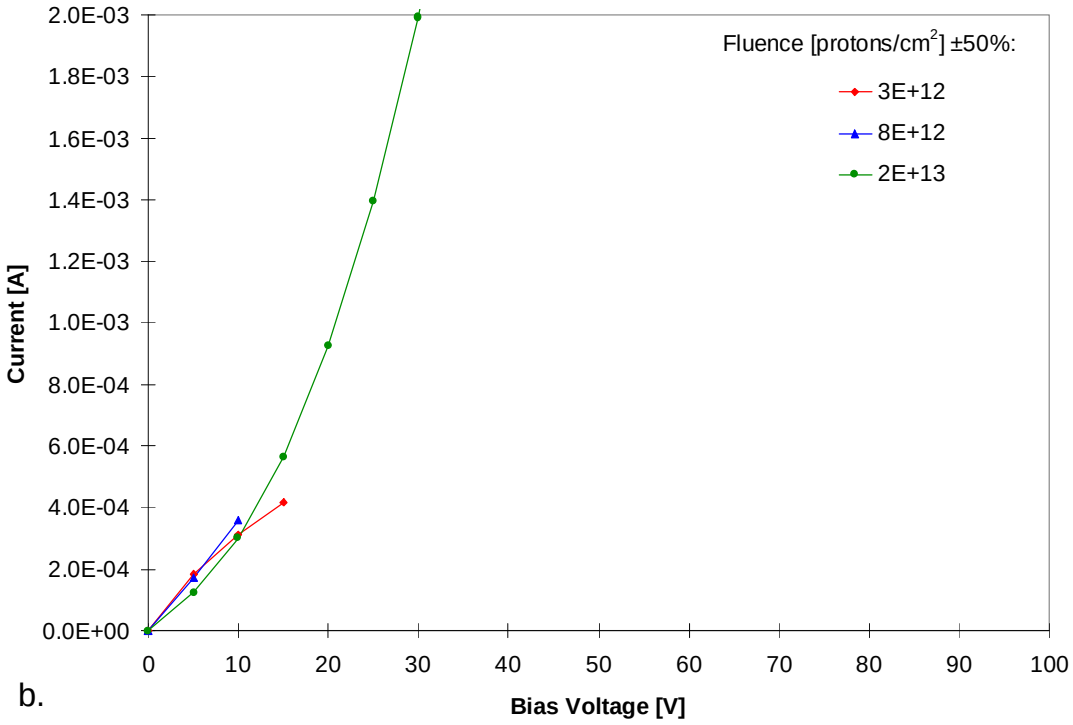

b.

Figure 4: F-disk detector 1295-15 VI curves for different fluences. a) Bias current. b) Guard ring current.

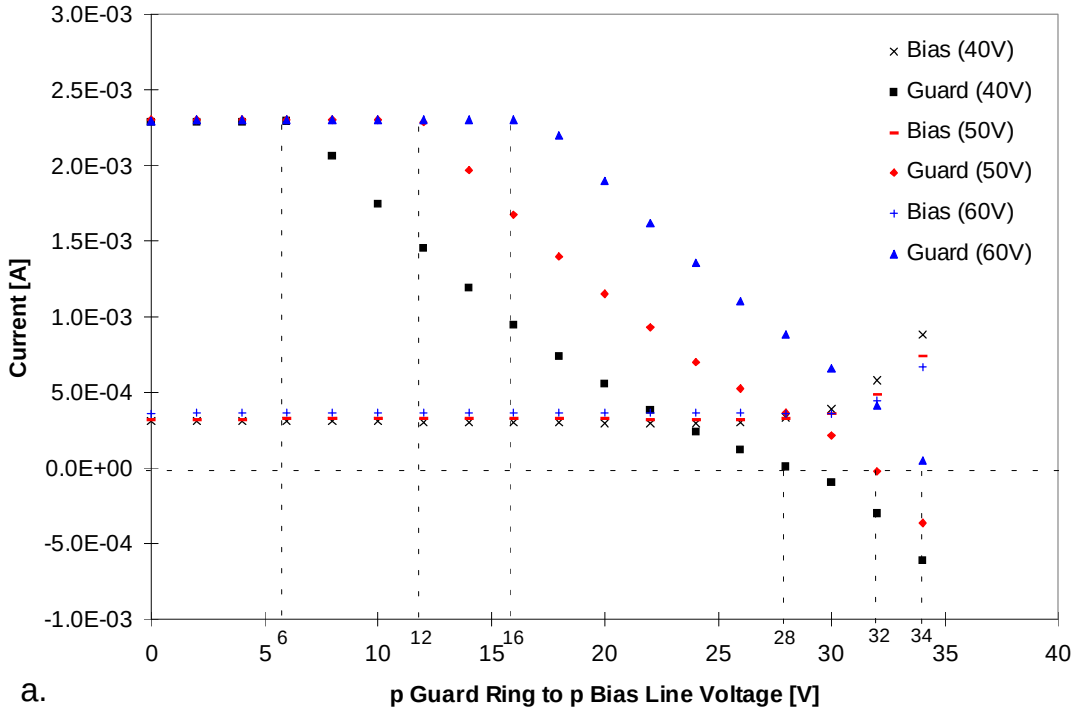

a.

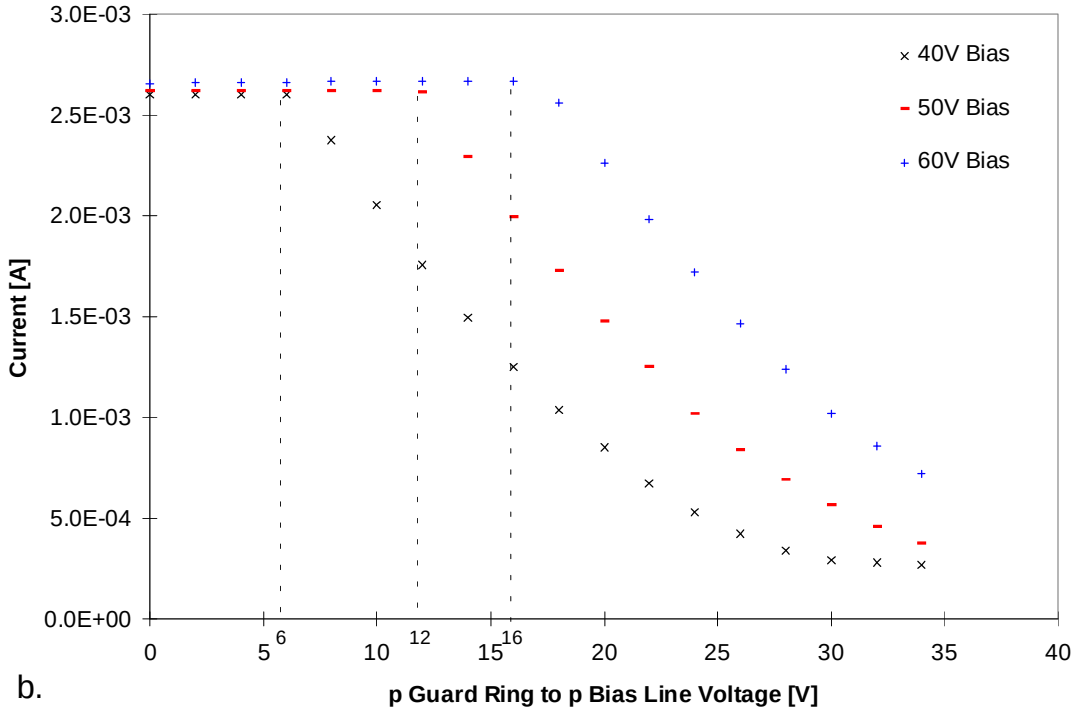

b.

Figure 5: F-disk detector currents as function of guard to bias line voltage, for different bias voltages, after irradiation. a) Individual currents. b) Total current (bias + guard).

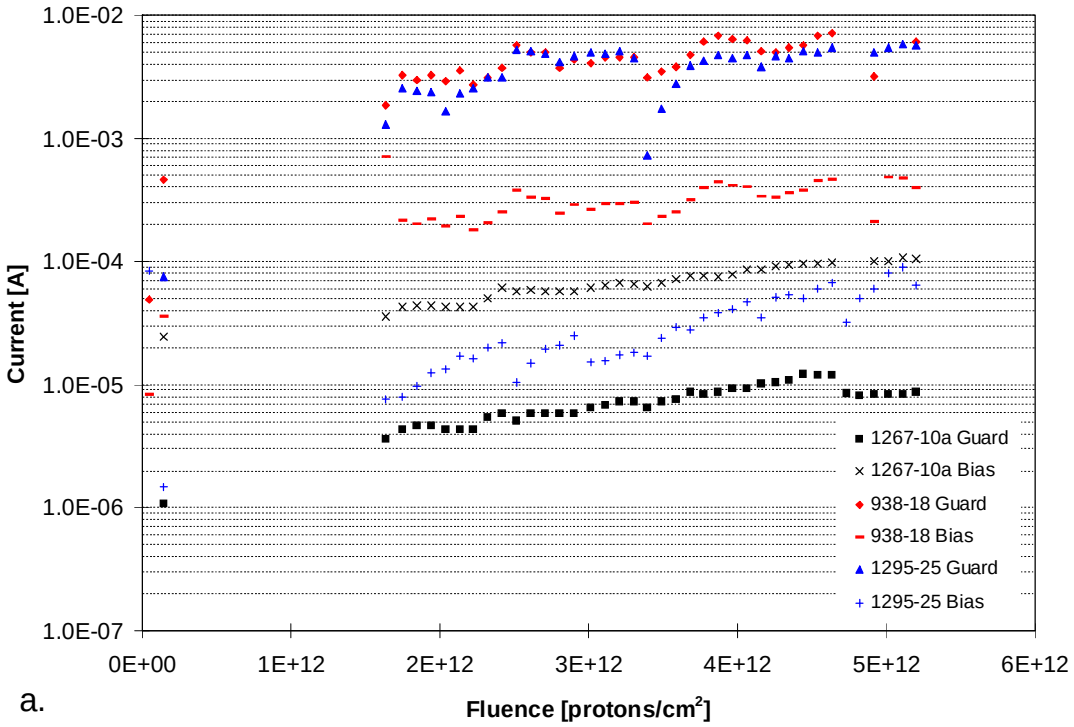

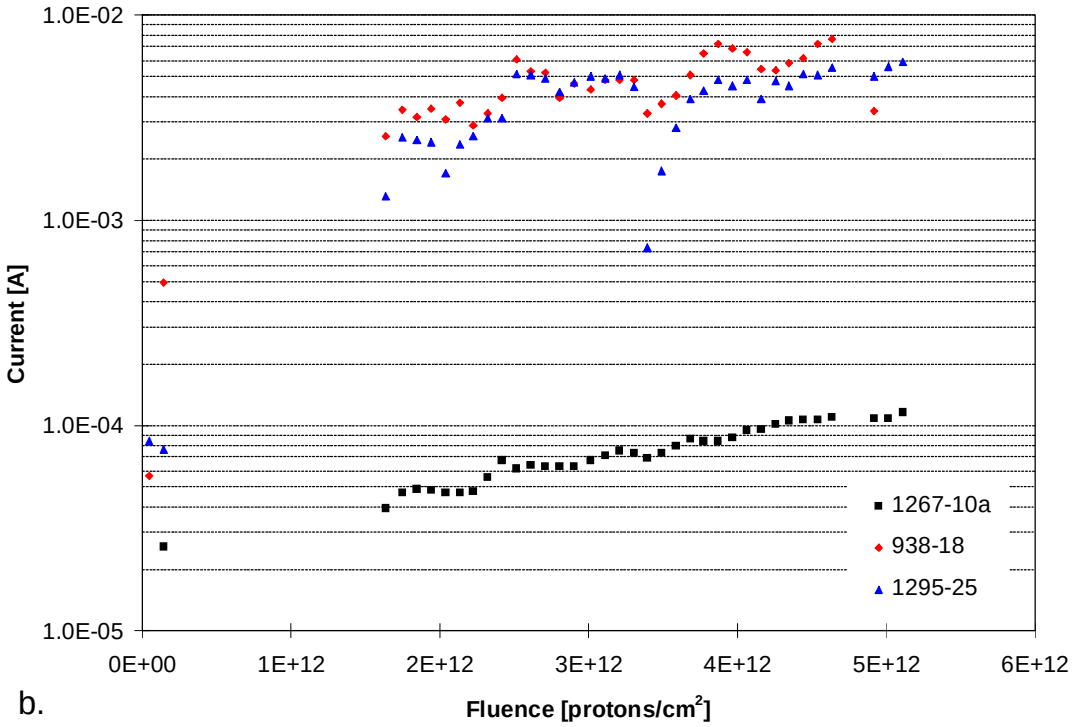

Figure 6: Increase in leakage currents with fluence for the detectors irradiated in the first February exposure. a) Individual currents. b) Total currents (bias + guard).

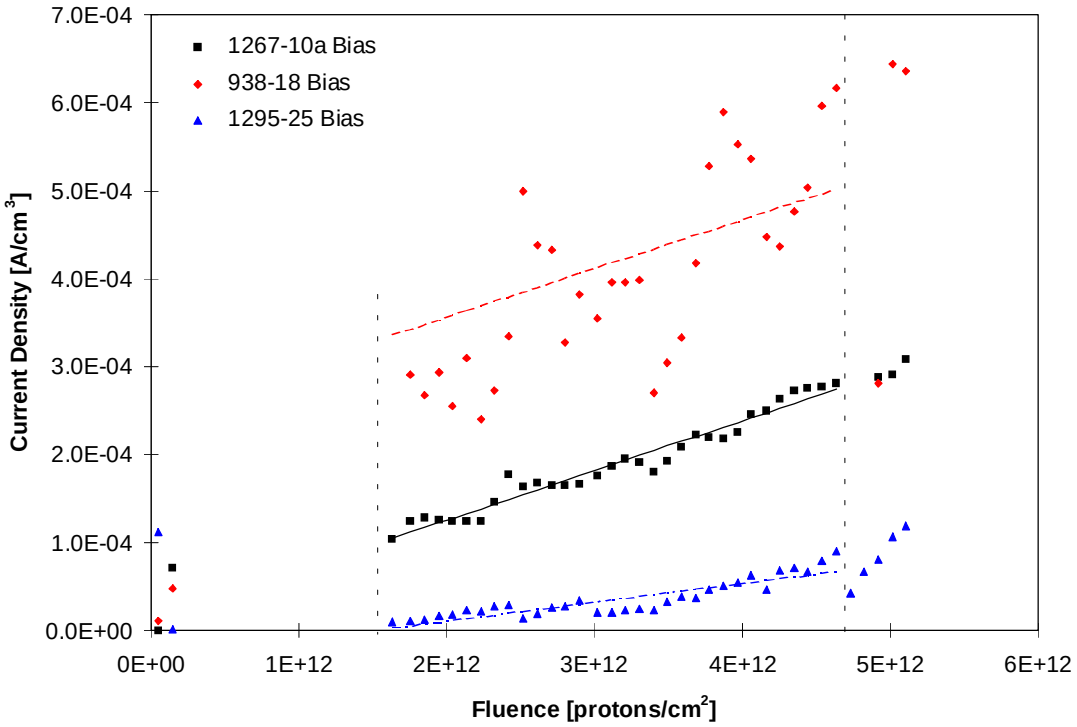

Figure 7: Bias current densities (by detector volume) for the detectors irradiated in the first February exposure. The lines correspond to least square fits using the points between the dotted lines. The slope of the fit is defined as the long term damage rate

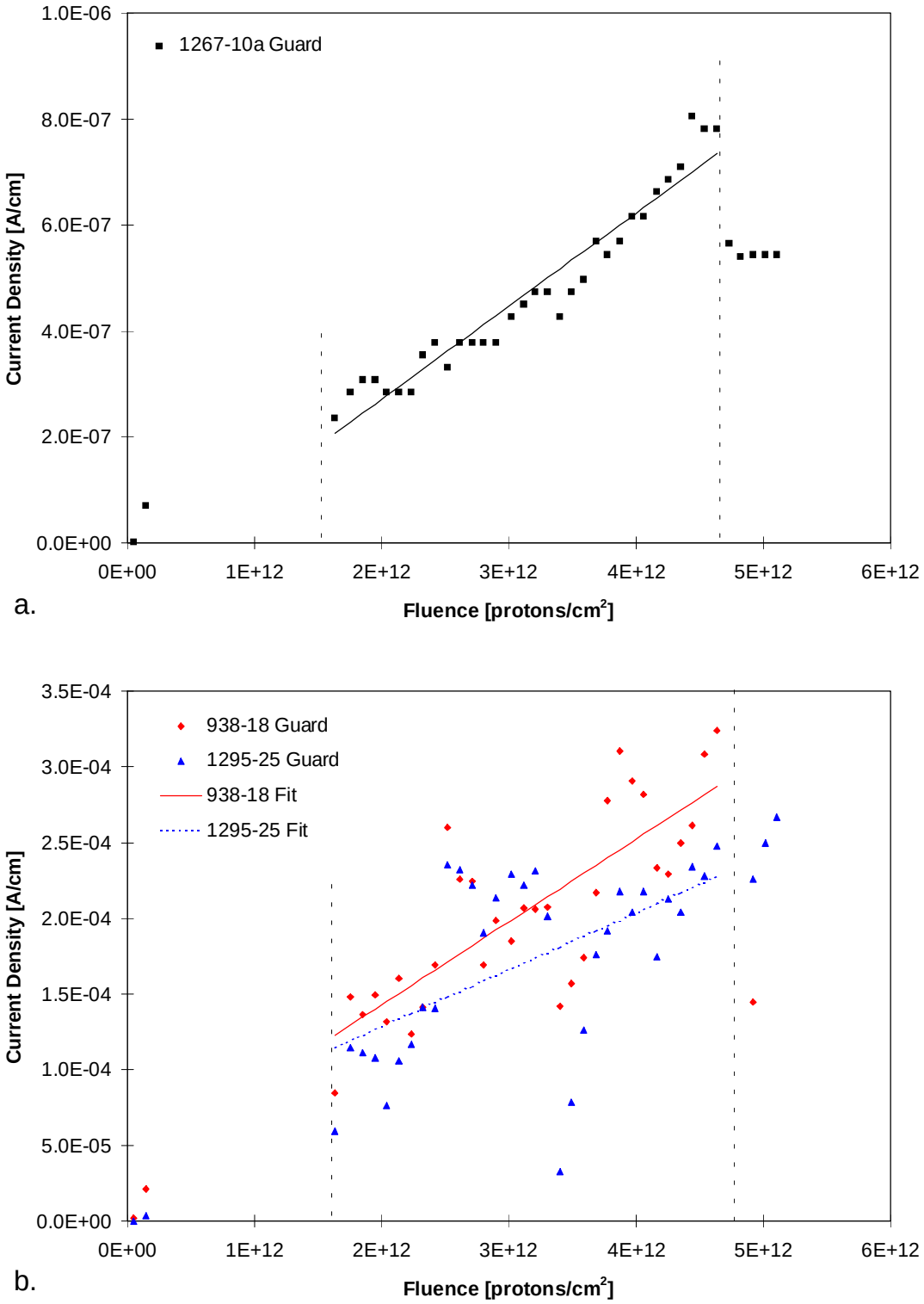

Figure 8: Guard ring current densities (by guard ring length) for the detectors irradiated in the first February exposure. The lines correspond to least square fits using the points between the dotted lines. The slope of the fit is defined as the long term damage rate shown in Table 1. a) Barrel detector. b) F-disk detectors.

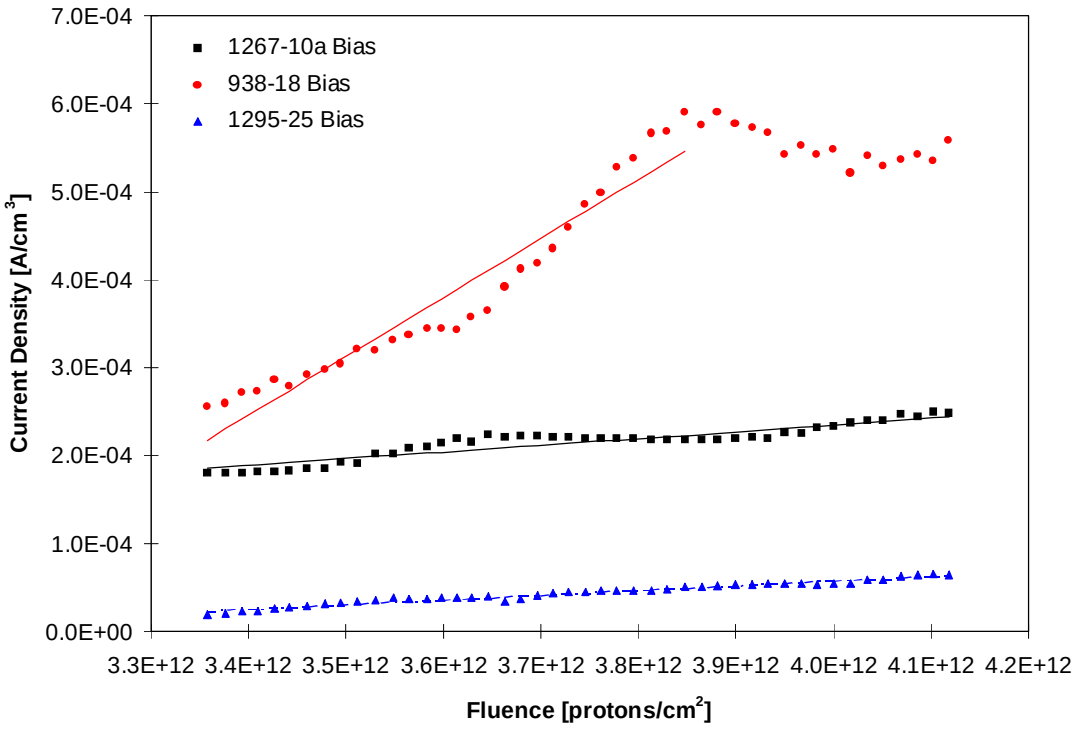

Figure 9: Bias current densities (by det. volume) for the detectors irradiated in the first February exposure, in a fluence interval where the fast component of the damage is clearly visible. The lines correspond to least square fits whose slope is defined as the short term damage rate shown in Table 1.

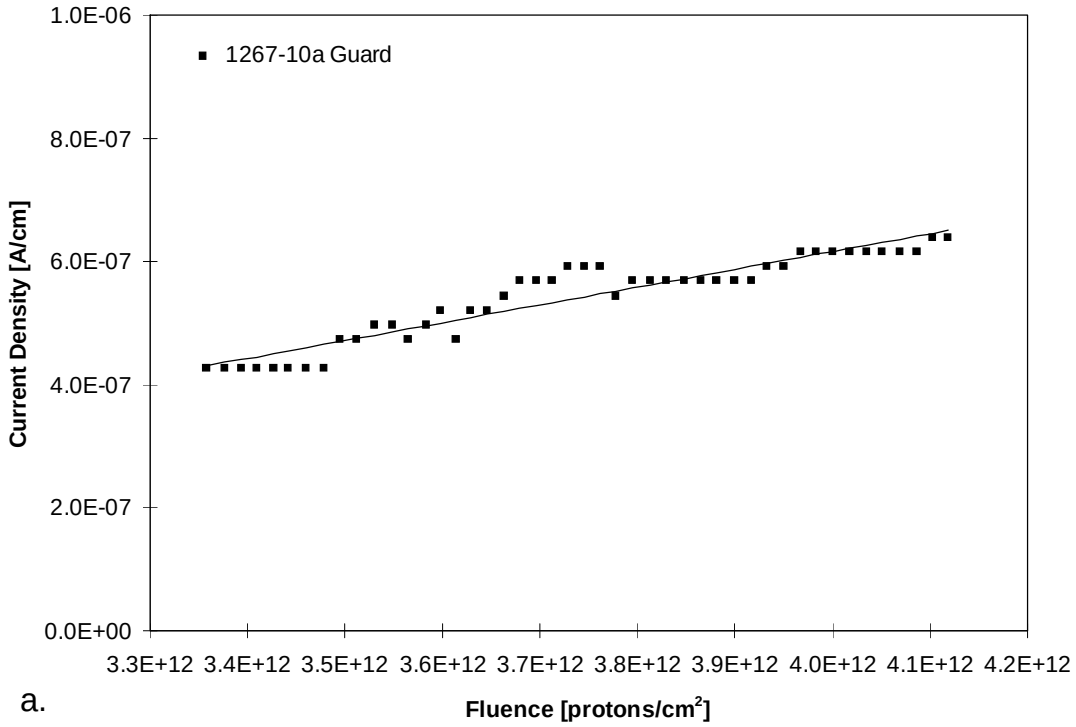

a.

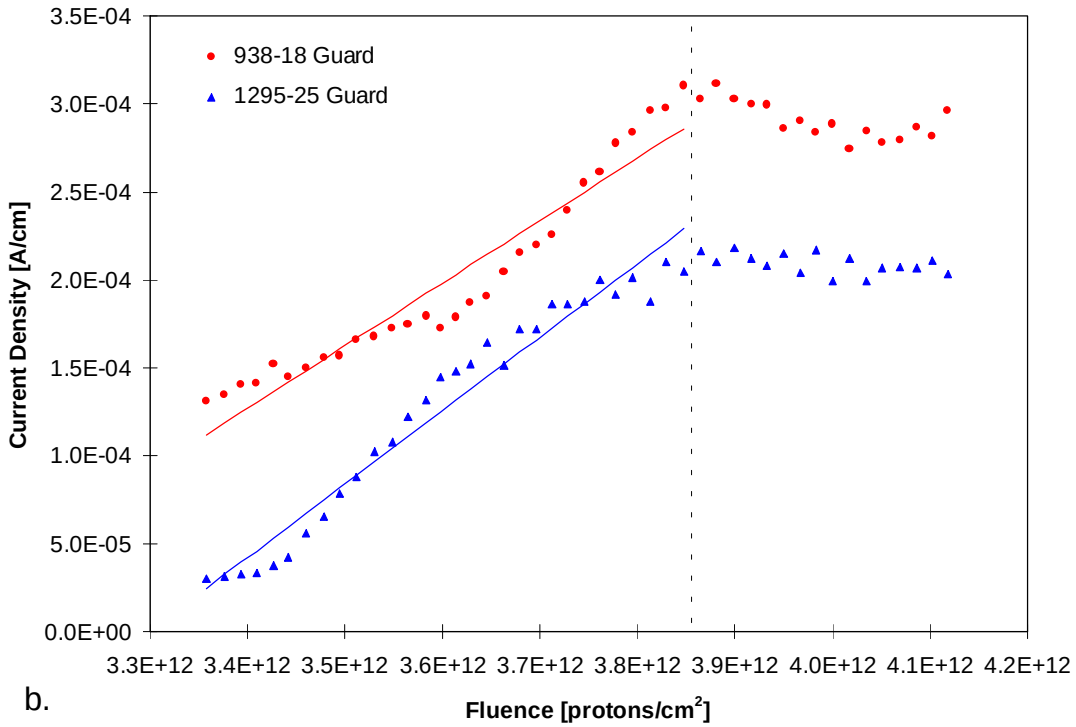

b.

Figure 10: Guard ring current densities (by guard ring length) for the detectors irradiated in the first February exposure, in a fluence interval where the fast component of the damage is clearly visible. The lines correspond to least square fits using the points to the left of the dotted line. The slope of the fit is defined as the short term damage rate shown in Table 1. a) Barrel detector. b) F-disk detectors.

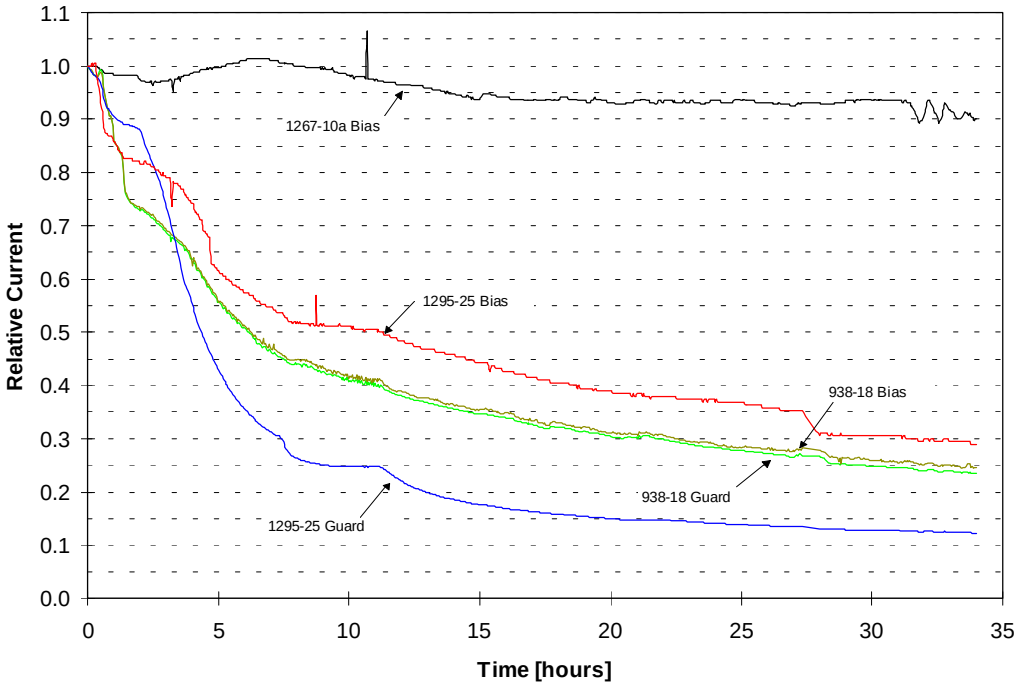

Figure 11: Evolution of the leakage currents of the detectors irradiated in the first February exposure at 5°C, after the last period of irradiation (fluence of 5.2×10^{12} protons/cm2, 139 Krad), sampled every 2.5 minutes. All currents are shown normalized to their initial values (at t=0).

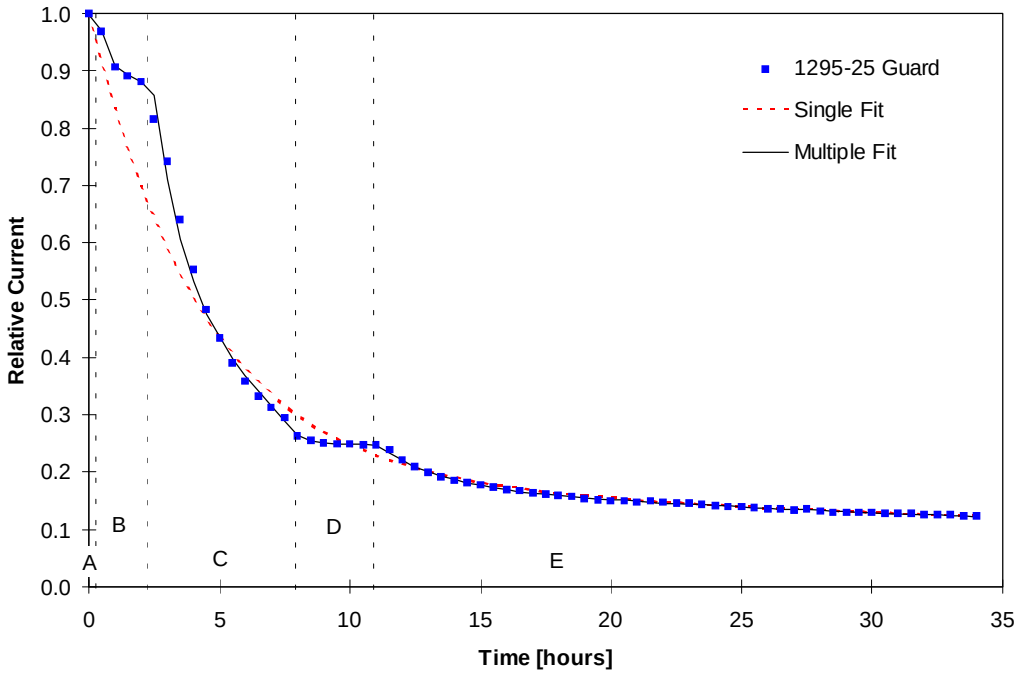

Figure 12: Fits to the annealing of the 1295-25 guard ring current from Figure 11. Both fits use the sum of two exponentials, the single fit has parameters that are independent of time, while the multiple fit has five sets of parameters, each set for a different time interval (A through E). See Table 2 for the parameters. The data set used for the fits had 10 times more points than those shown.

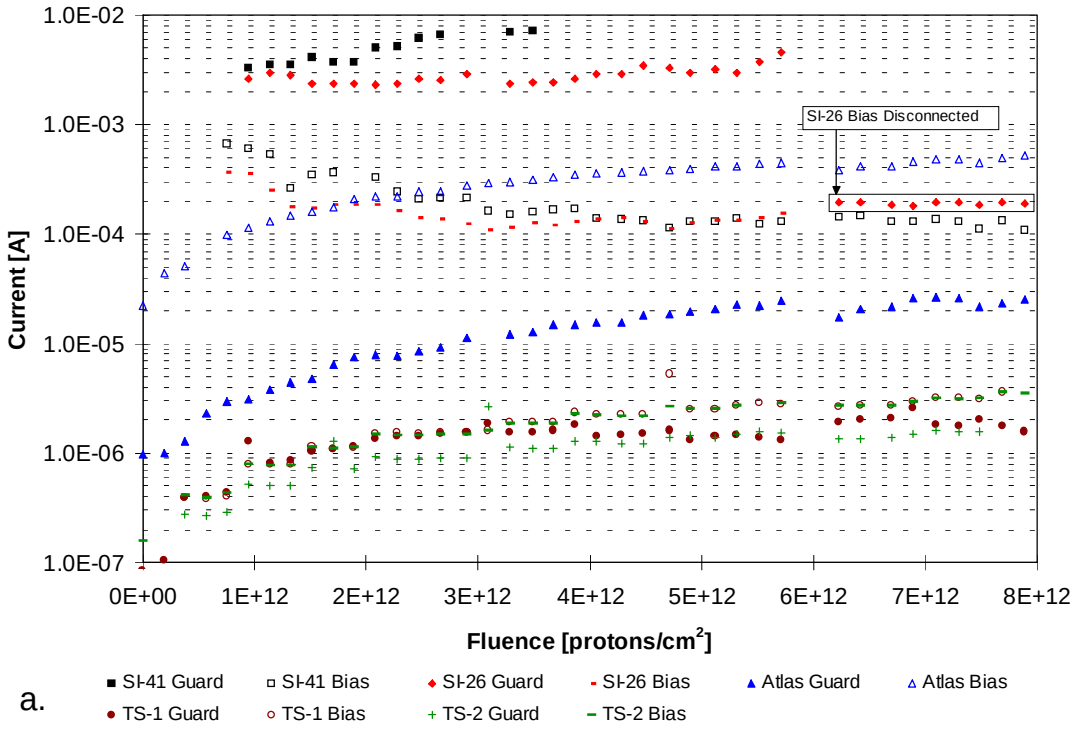

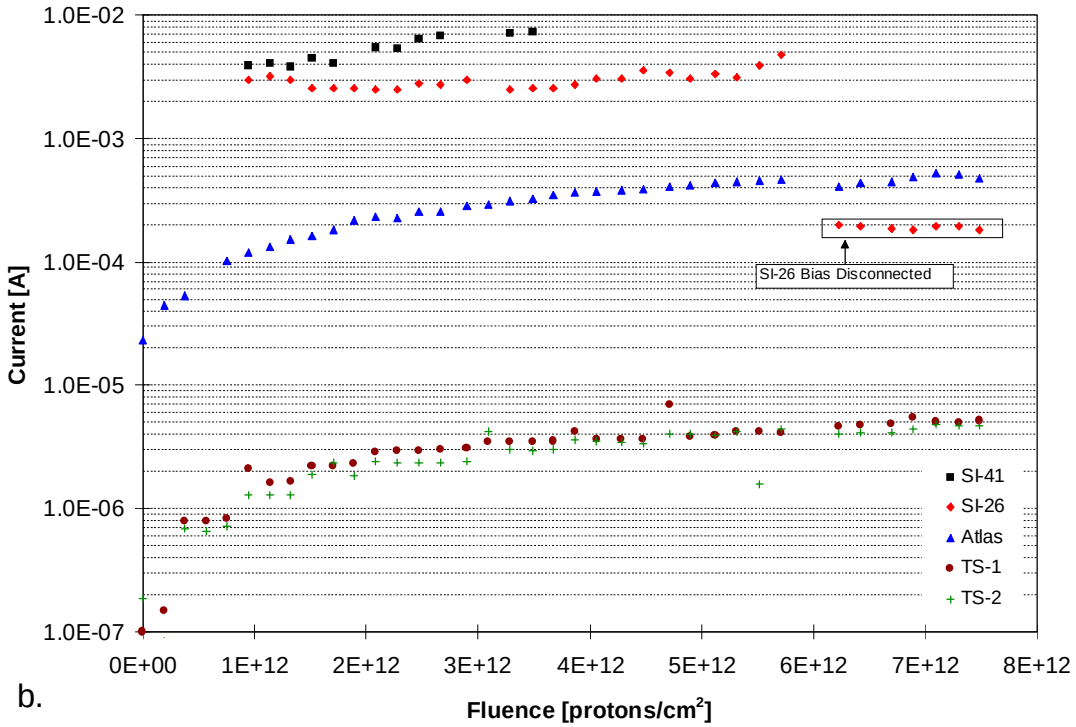

Figure 13: Increase in leakage currents with fluence for the detectors irradiated in the second February exposure. a) Individual currents. b) Total currents (bias + guard).

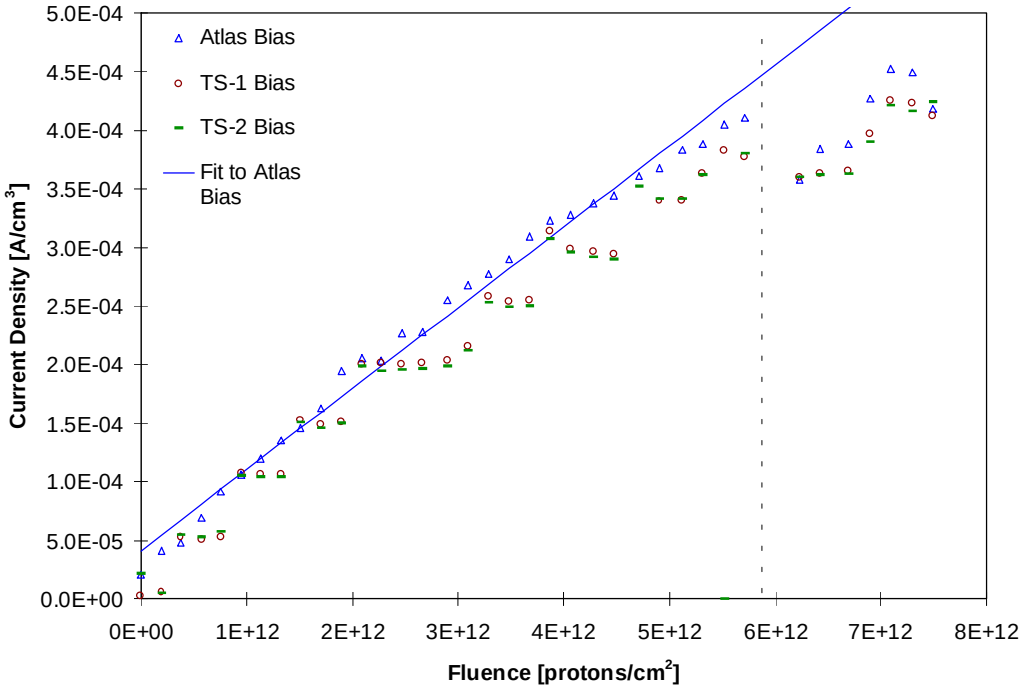

Figure 14: Bias current densities (by det. volume) for the Atlas detector and test structures. The fit has a slope of 6.9×10^{-17} A/cm (long term damage rate) and included all the points to the left of the dotted line.

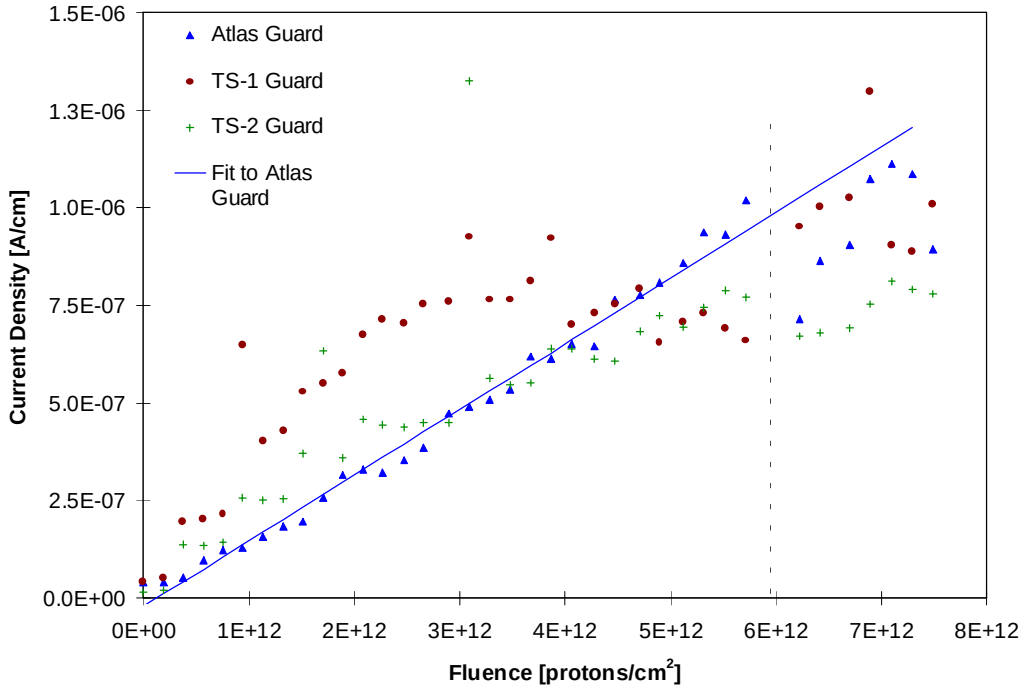

Figure 15: Guard ring current densities (by guard ring length) for the Atlas detector and test structures. The fit has a slope of 1.7×10^{-19} A.cm (long term damage rate) and includes all points to the left of the dotted line.

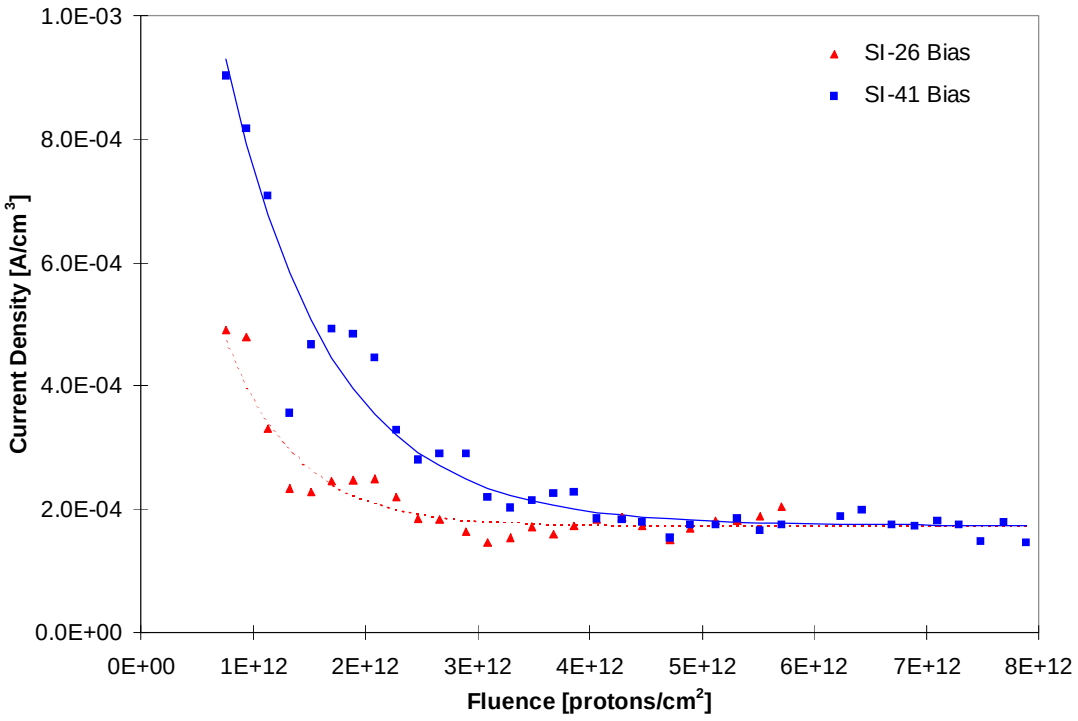

Figure 16: Evolution of the bias current density (by det. volume) with fluence for the SINTEF prototype detectors. The lines correspond to least square fits to equations 4 and 5.

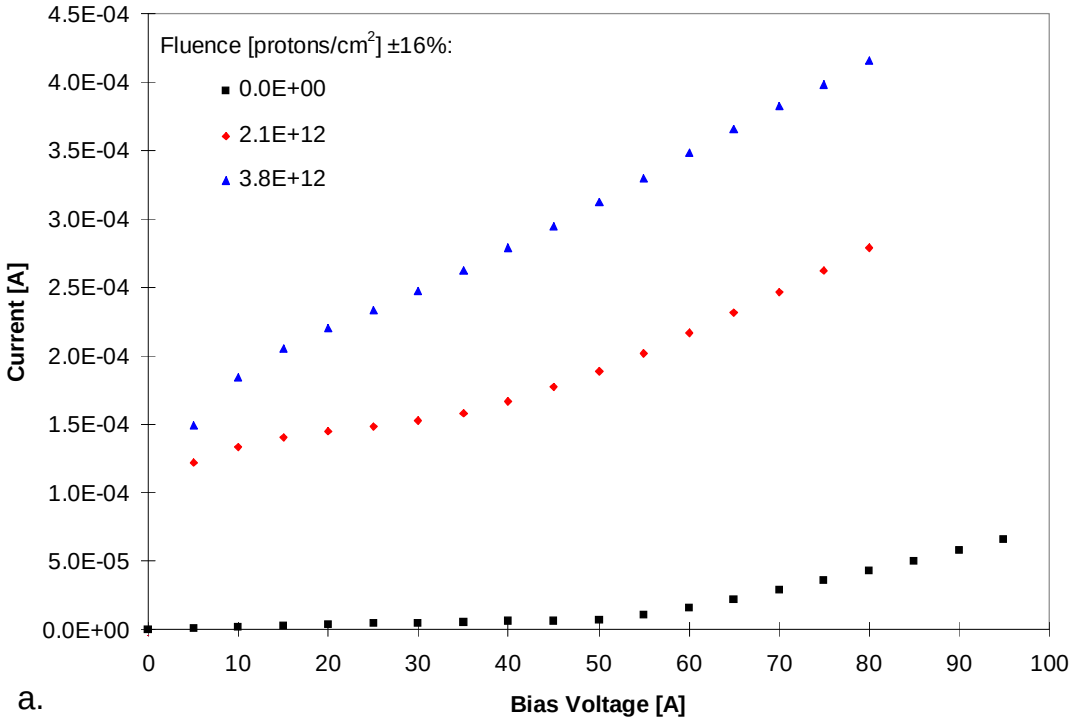

a.

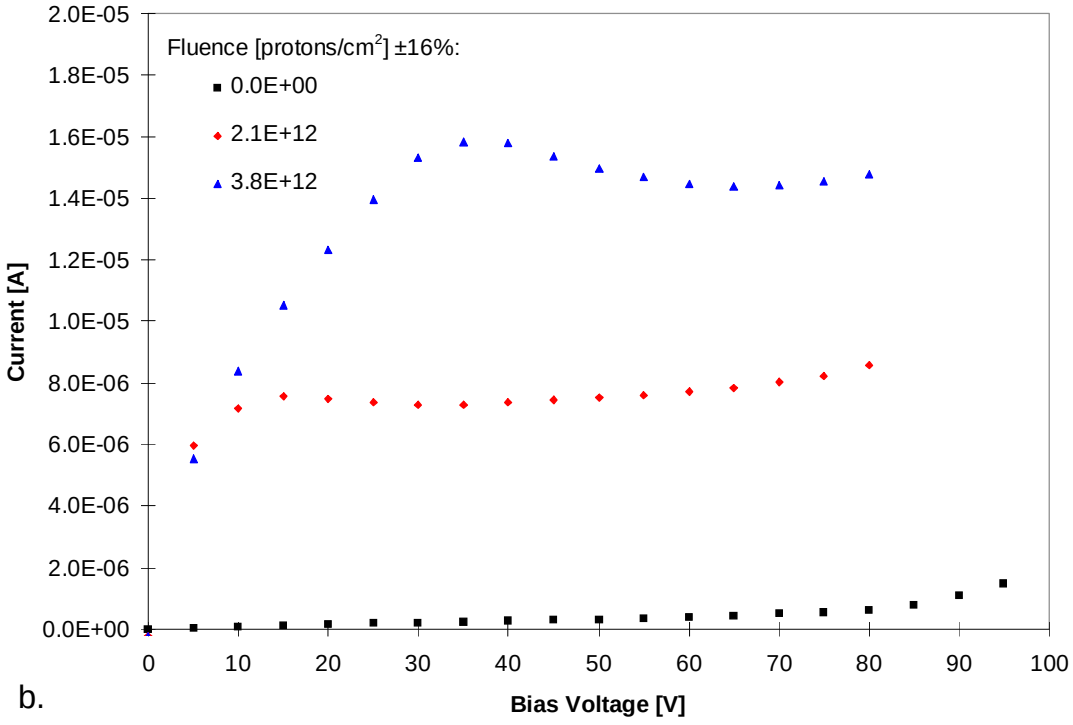

b.

Figure 17: Atlas detector VI curves for different fluences. a) Bias current b) Guard ring current..

Erratum to DØ Note 2911

Rafael Gómez
Fermilab / Universidad de Los Andes

In DØ Note 2911 titled "Effects of Radiation on the Leakage Currents of Silicon Microstrip Detectors for the H and F-Disks of the DØ Silicon Tracker," there is an error in section 4 ("Expected Dose for the F-Disks", page 11). This section should read as follows:

4. Expected Dose for the F-Disks

In DØ Note 2679 [5] the charged particle and neutron fluxes during Run II was estimated. For the F-disks we will use half the charged particle flux because the low momentum particles will not traverse the disks more than once as they do with the barrels. Hence, the charged particle flux is given by:

$$\phi_{ch}(r_\perp) \cong \frac{5.95 \times 10^{10}}{r_\perp^2} \text{cm}^{-2}/\text{pb}^{-1} \tag{6}$$

where $r_\perp$ is the distance perpendicular to the beam direction. If we integrate this flux over the whole disk coverage (from an inner radius of 2.54 cm to an outer radius of 9.84 cm) and divide by the area, we get the following average flux:

$$\phi_{ch} \cong 1.8 \times 10^{9}\ \text{cm}^{-2}/\text{pb}^{-1} \tag{7}$$

And the neutron flux is:

$$\phi_{n} \cong 1.8 \times 10^{9}\ \text{cm}^{-2}/\text{pb}^{-1} \tag{8}$$

This means that with the Tevatron running at an approximate integrated luminosity of 2000 pb^{-1}/year [5] the fluences will be:

$$\phi_{ch} \cong 3.6 \times 10^{12}\ \text{cm}^{-2}/\text{year} \tag{9}$$

for charged hadrons, and

$$\phi_{n} \cong 3.6 \times 10^{12}\ \text{cm}^{-2}/\text{year} \tag{10}$$

for neutrons.

These fluxes are accurate to within a factor of 2 because they do not take into account other particles, like gammas, electrons, etc. and processes like beam-gas collisions or Tevatron beam losses.